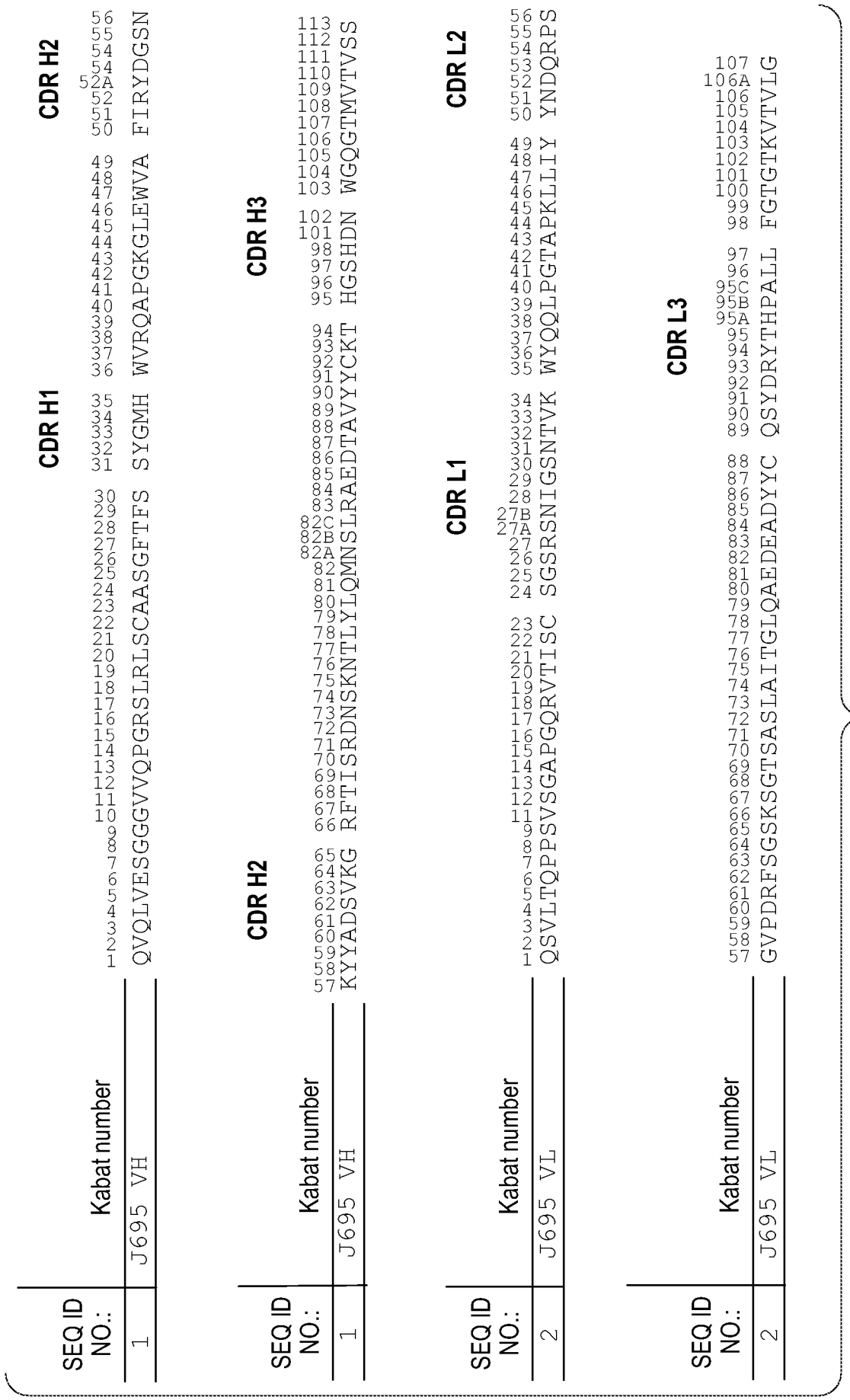
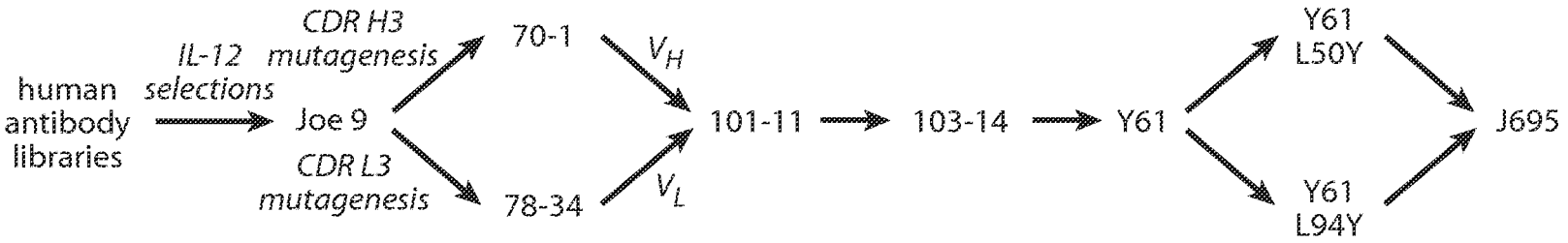

CDR H1
CDR H2
CDR H3
CDR L1
CDR L2
CDR L3
SEQ ID NO.:
Kabat number
1
J695 VH
QVQLVESGGGVVQPGRSLRLSCAASGFTFS SYGMH WVRQAPGKGLEWVA FIRYDGSN KYYADSVKG RFTISRDNSKNTLYLQMNSLRAEDTAVYYCKT HGSHDN WGQGTMVTVSS
2
J695 VL
QSVLTQPPSVSGAPGQRVTISC SGSRSNIGSNTVK WYQQLPGTAPKLLIY YNDQRPS GVPDRFSGSKSGTSASLAITGLQAEDEADYYC QSYDRYTHPALL FGTGTKVTVLG

Fig. 1



mAb	Partial CDR Sequence H*	H3	L1	L2	L3	k_{on} $M^{-1}s^{-1} \times 10^{-5}$	k_{off} $s^{-1} \times 10^{-5}$	K_D pM	RBA IC_{50} pM	PHA IC_{50} pM
	92 93 94	95 96 97 98 101 102	25 26 27	50 51	91 92 93 94 95 95A 95B 95C 96 97					
Joe9	C T T	S G S Y D Y	G G R	G N	Y D S S L R G S R V	ND	10,000	ND	1,500,000	1,000,000
70-1	. . .	H . . H . N	. . .	. .	. . . . .	0.94 ± 0.01	503 ± 105	53,900 ± 11,200	ND	200,000
78-34	. . .	. . . . .	. . .	. .	. . R G F T	ND	1,640	ND	200,000	600,000
101-11	. . .	H . . H . N	. . .	. .	. . R G F T	ND	450	ND	2,000	20,000
103-14	. K .	H . . H . N	. . .	. .	. E R G F T . . M .	ND	67	ND	40	1200
Y61	. K .	H . . H . N	. . .	. .	. . R G T H P A L L	3.91 ± 0.42	23.6 ± 1.7	604 ± 78	16	130
Y61 L50Y	. K .	H . . H . N	. S .	Y .	. . R G T H P A L L	5.05 ± 0.93	6.95 ± 1.38	138 ± 37	20	ND
Y61 L94Y	. K .	H . . H . N	. S .	. .	. . R Y T H P A L L	3.73 ± 0.46	12.7 ± 1.0	341 ± 49	60	50
J695	. K .	H . . H . N	. S .	Y .	. . R Y T H P A L L	5.03 ± 1.11	5.14 ± 0.48	102 ± 25	50	10

A dot (".") signifies that an antibody has the same residue at that position as Joe 9. The complete Joe 9 CDR sequences are: H1: ^{27}FTFSSYGMH^{35};H2: ^{50}FIRYDGSNKYYADSVKG^{65}; H3, ^{95}SGSYDY^{102};L1: ^{24}SGGRSNIGSNTVK^{34}; L2: ^{50}GNDQRPS^{56}; L3, ^{89}QSYDSSLRGSRV^{97}. The complete ABT-874 CDR sequences are: H1: ^{27}FTFSSYGMH^{35}; H2: ^{50}FIRYDGSNKYYADSVKG^{65}; H3: ^{95}HGSHDN^{102}; L1: ^{24}SGSRSNIGSNTVK^{34}; L2: ^{50}YNDQRPS^{56}; L3: ^{89}QSYDRYTHPALL^{97}. ABT-874 was previously referred to as J695. Kabat (Kabat, TT et al. 1991) numbering is followed. H* represents the three heavy-chain framework residues immediately preceding CDR H3 (^{92}CTT^{94} in Joe 9, ^{92}CKT^{94} in ABT-874). RBA: Receptor binding assay; PHA: phytohemagglutinin lymphoblast assay. Kinetic constants with 95% confidence limits reported are from four determinations. ND: Not determined. Most of the data in this table are taken from (Salfeld, Roguska et al. 2000).

Fig. 2

SUBSTITUTE SHEET (RULE 26)

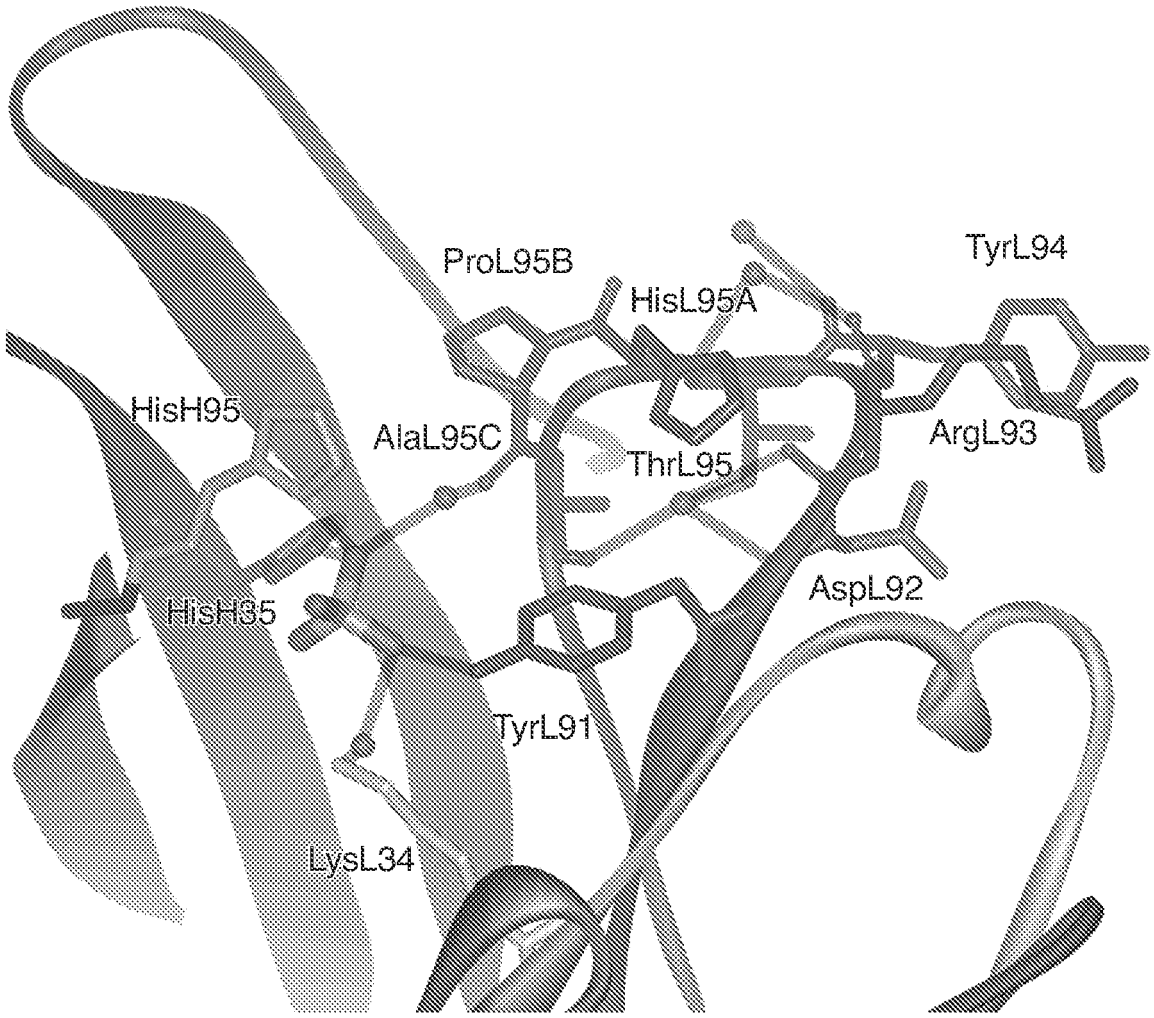

ProL95B
HisL95A
TyrL94
HisH95
AlaL95C
ThrL95
ArgL93
AspL92
HisH35
TyrL91
LysL34

Fig. 3

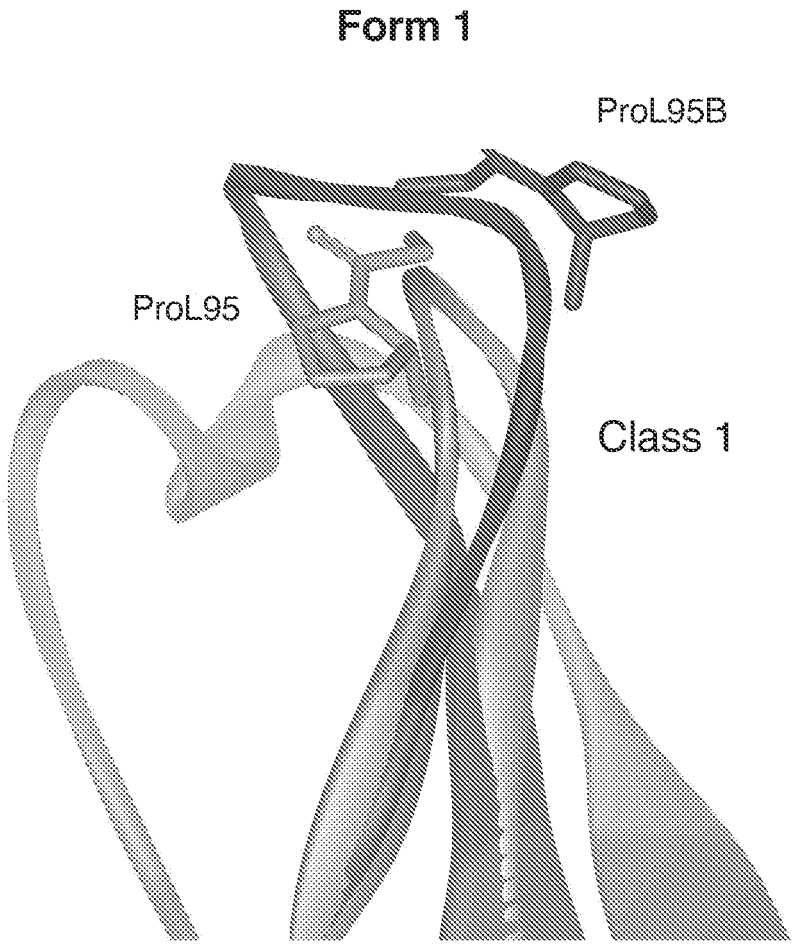


Fig. 4

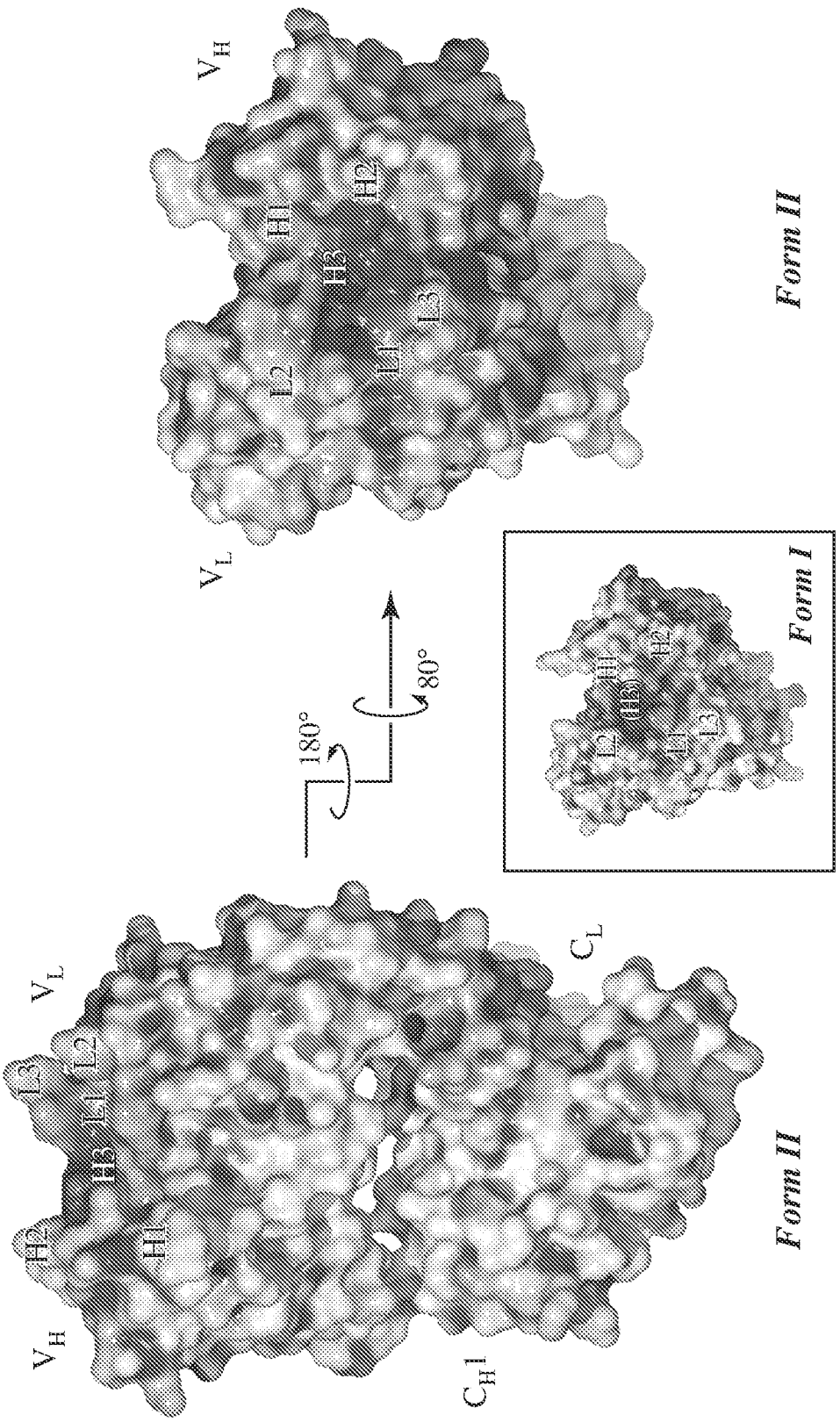


Fig. 5

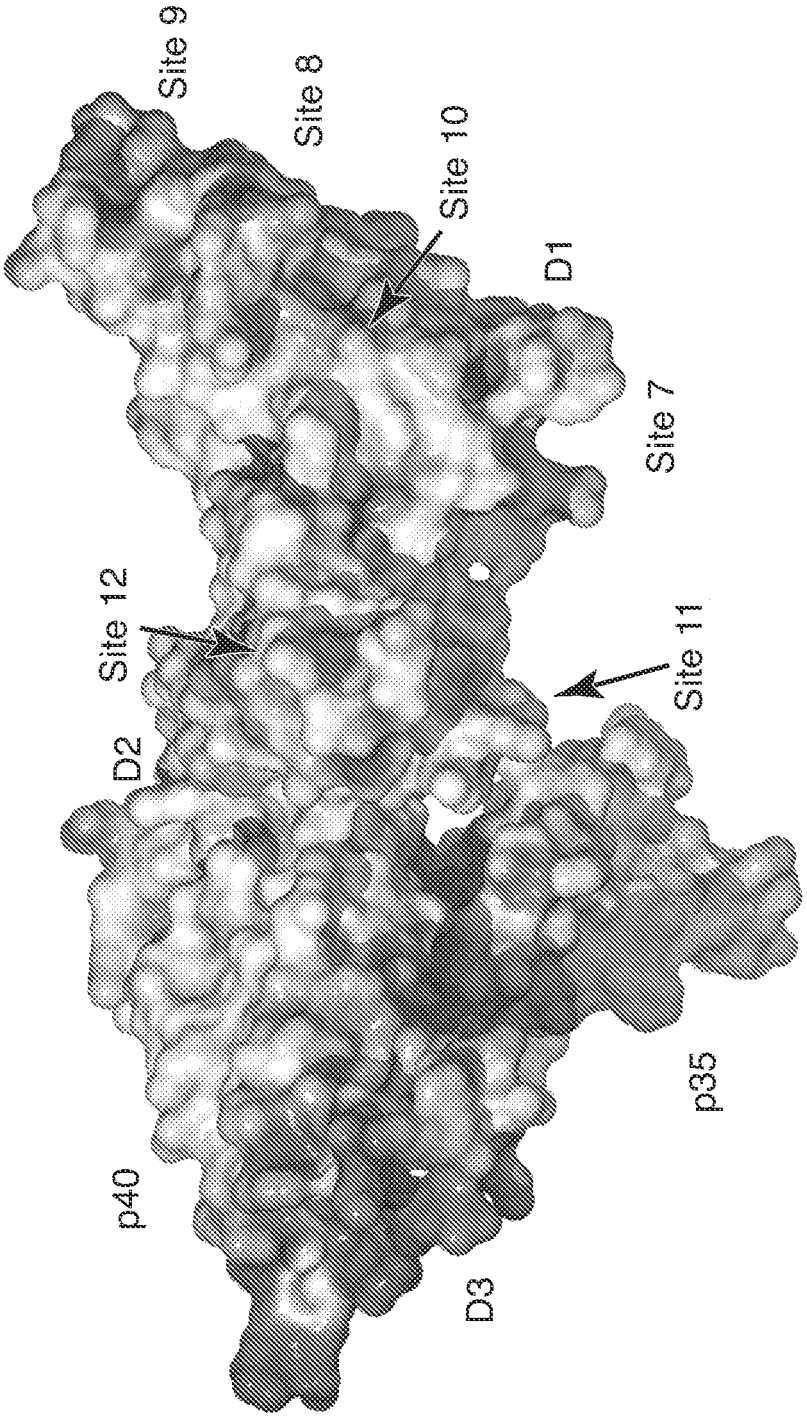


Fig. 6

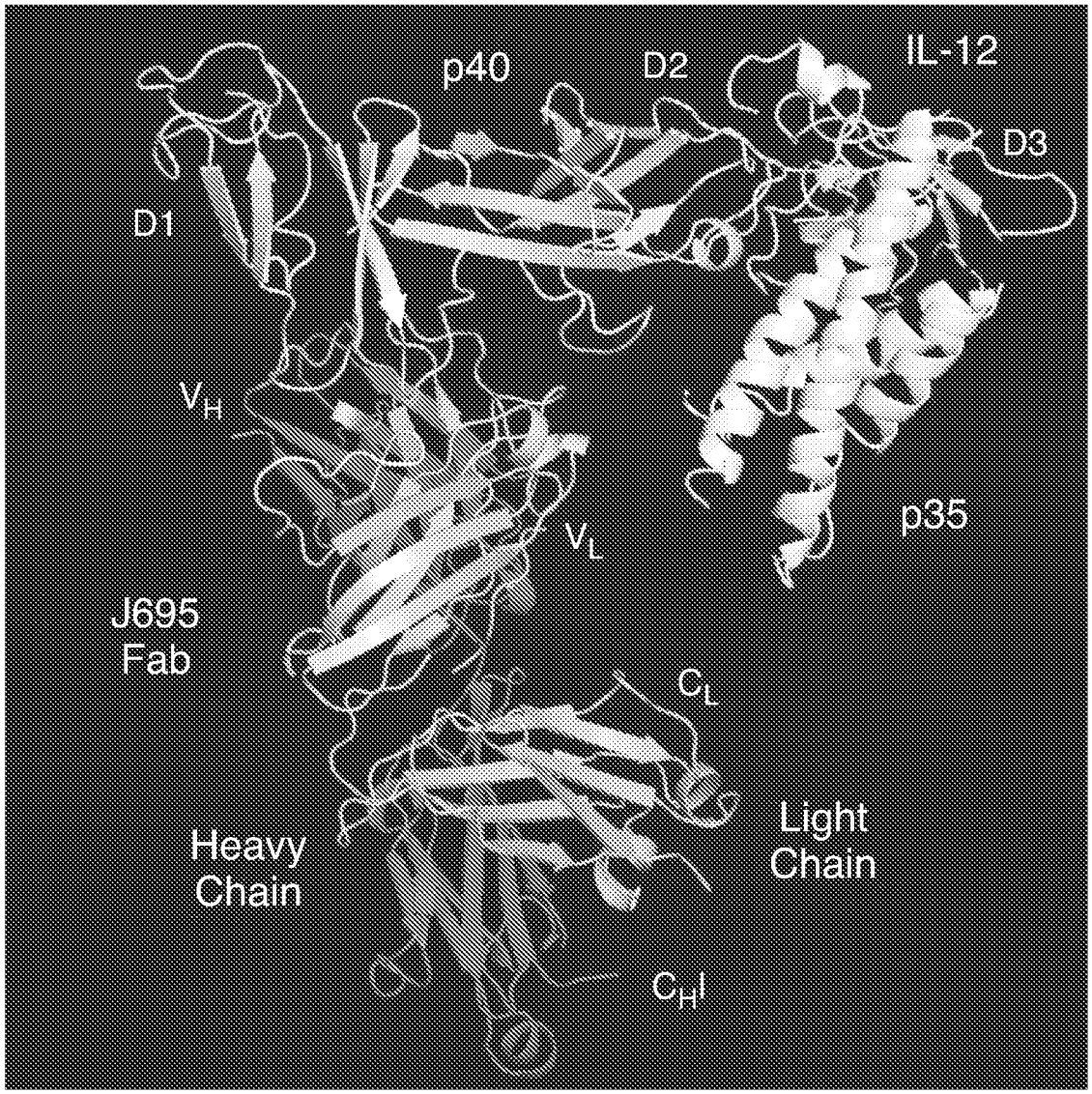

p40
D2
IL-12
D3
D1
V_H
V_L
p35
J695
Fab
C_L
Heavy
Chain
Light
Chain
$C_{H}I$

Fig. 7

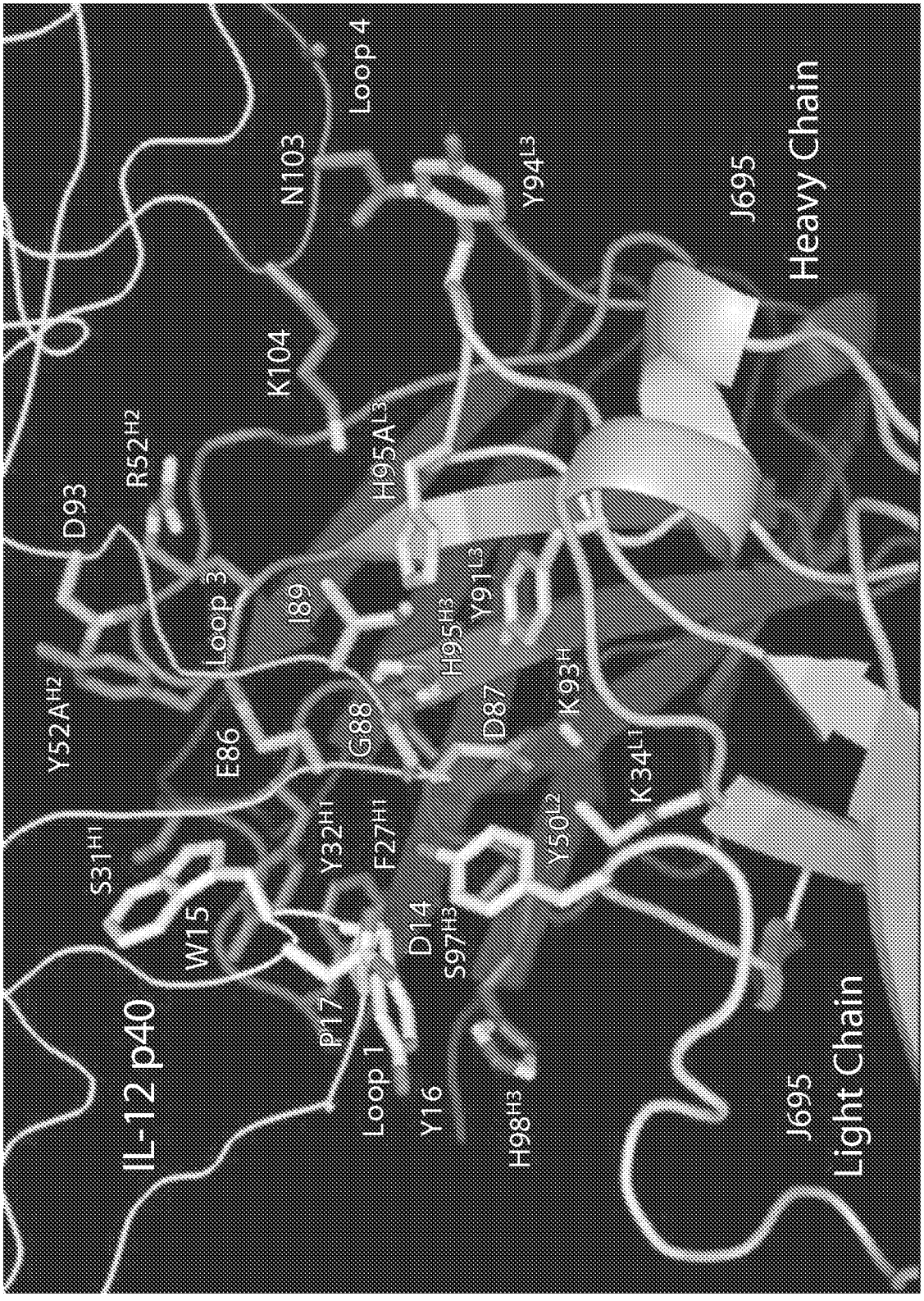

IL-12 p40
Y52A^{H2}
S31^{H1}
W15
P17
Loop 1
Y16
H98^{H3}
D93
R52^{H2}
E86
Loop 3
Y32^{H1}
F27^{H1}
D14
S97^{H3}
I89
G88
H95^{H3}
D87
Y50^{L2}
K104
N103
H95A^{L3}
Y91^{L3}
K93^{H}
K34^{L1}
Loop 4
Y94^{L3}
J695
Heavy Chain
J695
Light Chain

Fig. 8

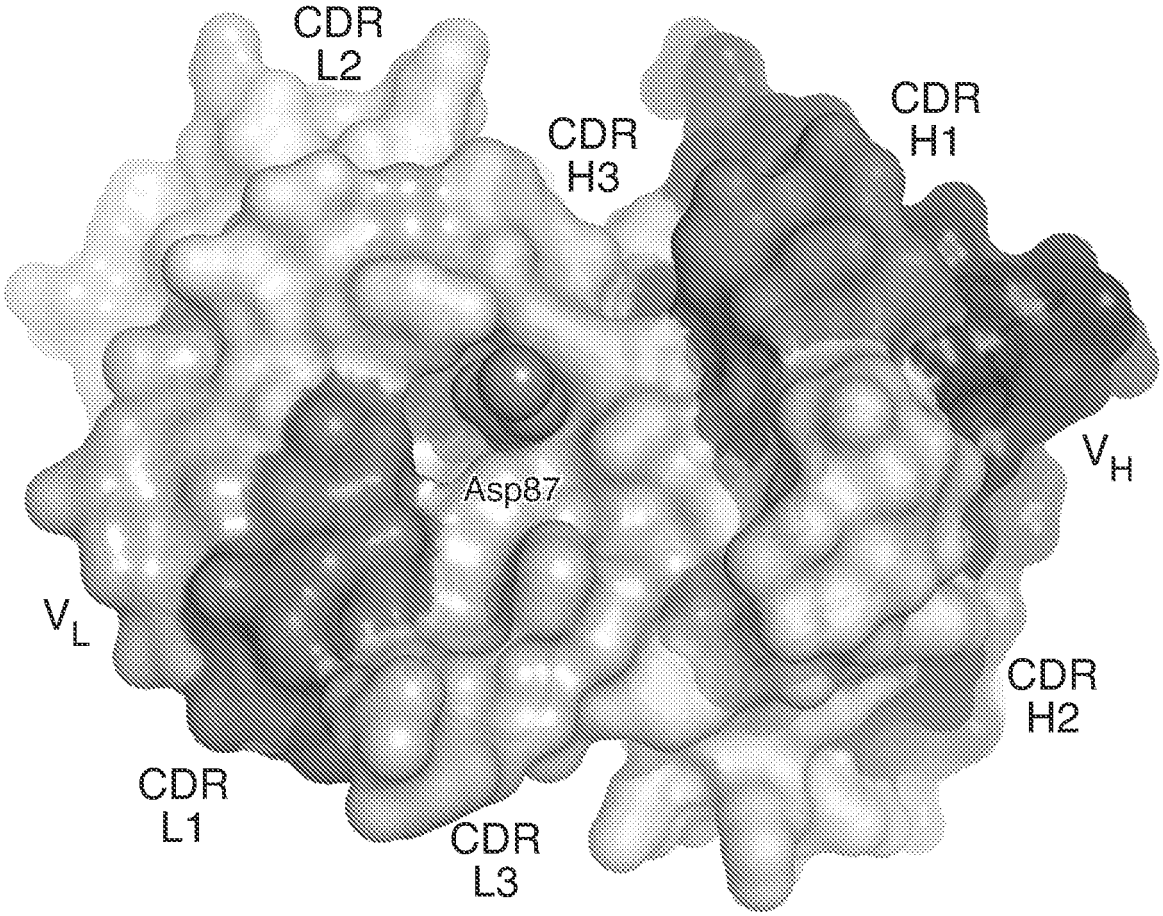


Fig. 9

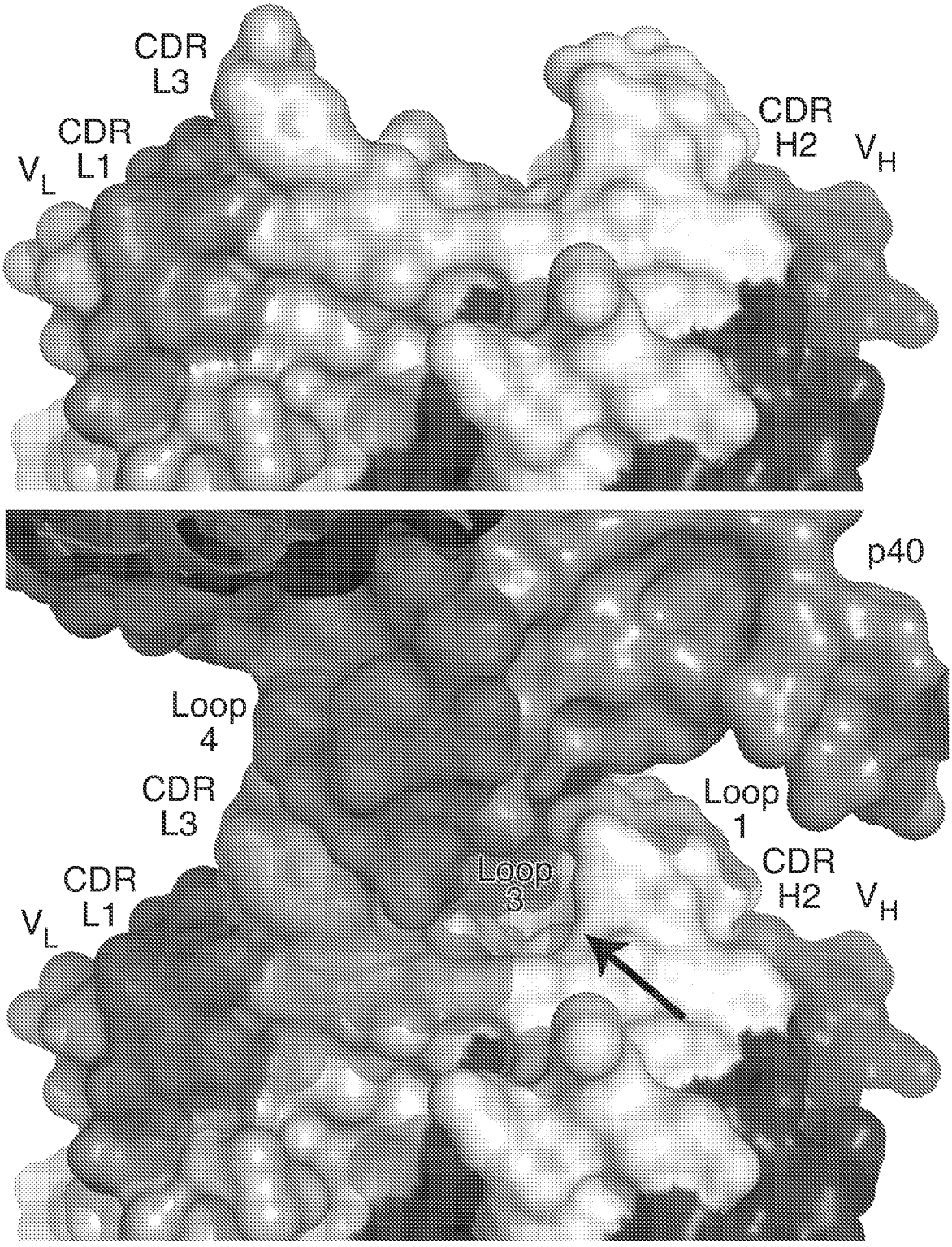

CDR
L3
CDR
L1
V_L
CDR
H2
V_H
p40
Loop
4
CDR
L3
CDR
L1
V_L
Loop
3
Loop
1
CDR
H2
V_H

Fig. 10

IL-12 p40 Sites Defined by Chimera Mapping

Site 7:	Site 8:	Site 9:	Site 10:	Site 11:	Site 12:
➢ Tyr16	➢ Leu40	➢ Gly35	➢ Gly61	➢ Asp97	➢ Arg157
➢ Asp87	➢ Asp41			➢ Gln98	➢ Val158
➢ Asp93	➢ Gln42			➢ Lys99	➢ Arg159
	➢ Ser43			➢ Glu100	➢ Gly160
	➢ Ser44			➢ Pro101	➢ Asp161
	➢ Glu45				➢ Asn162
	➢ Val46				➢ Lys163
	➢ Leu47				➢ Glu164

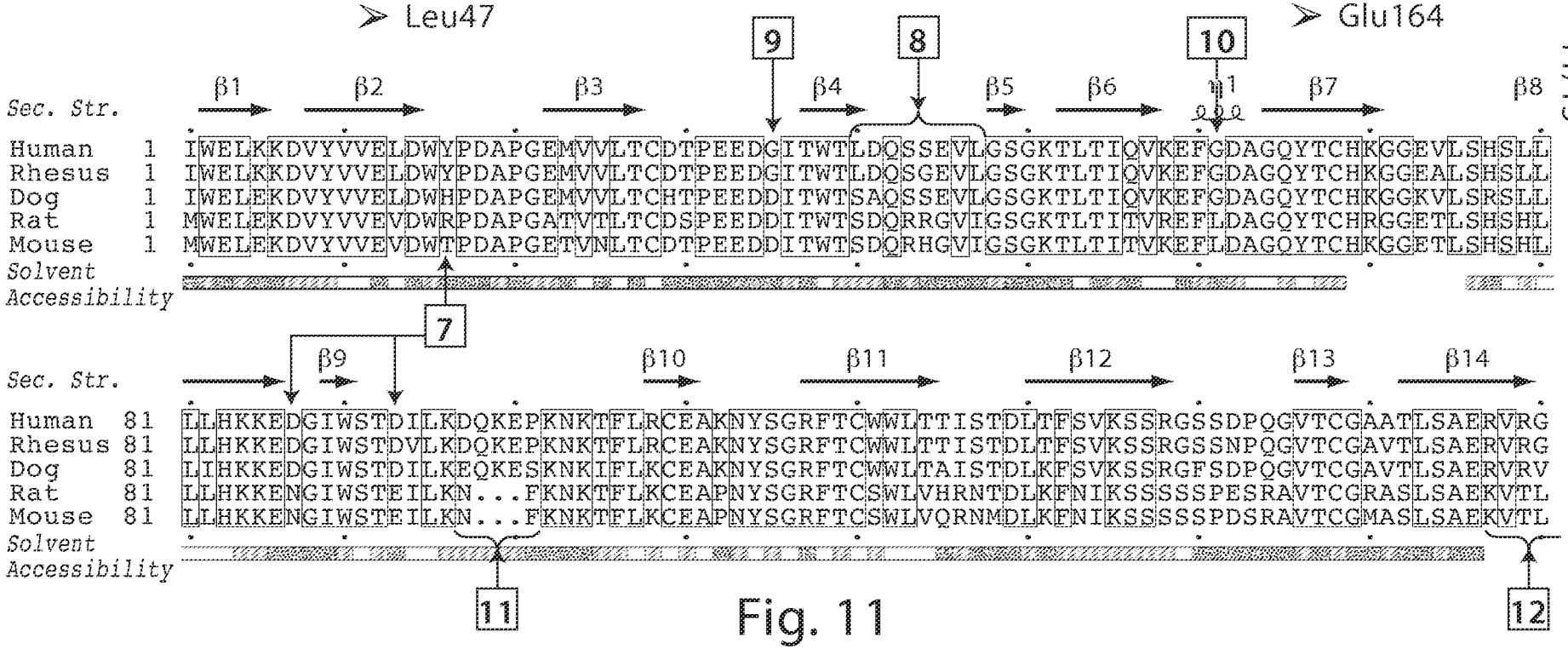


Fig. 11

SUBSTITUTE SHEET (RULE 26)

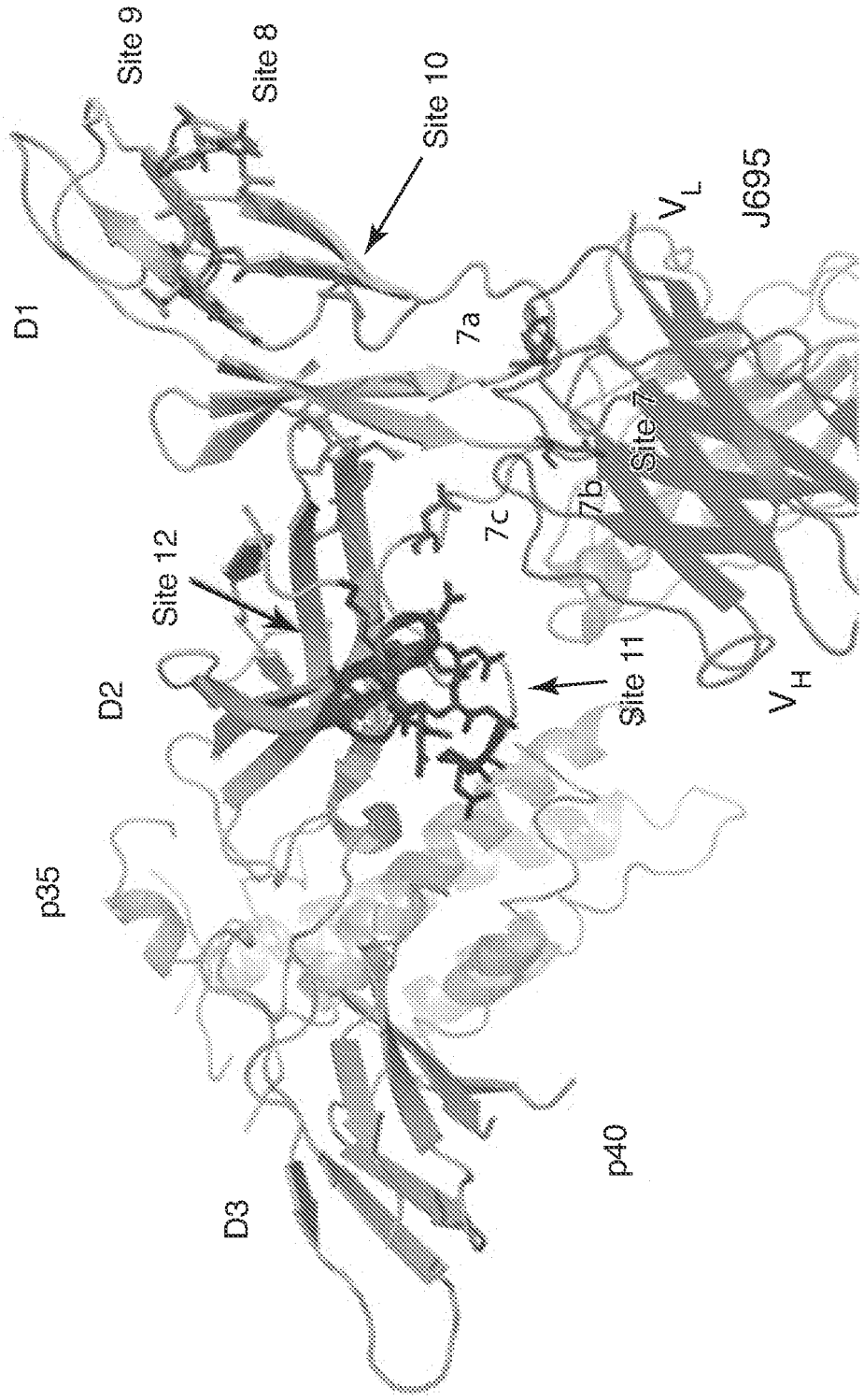
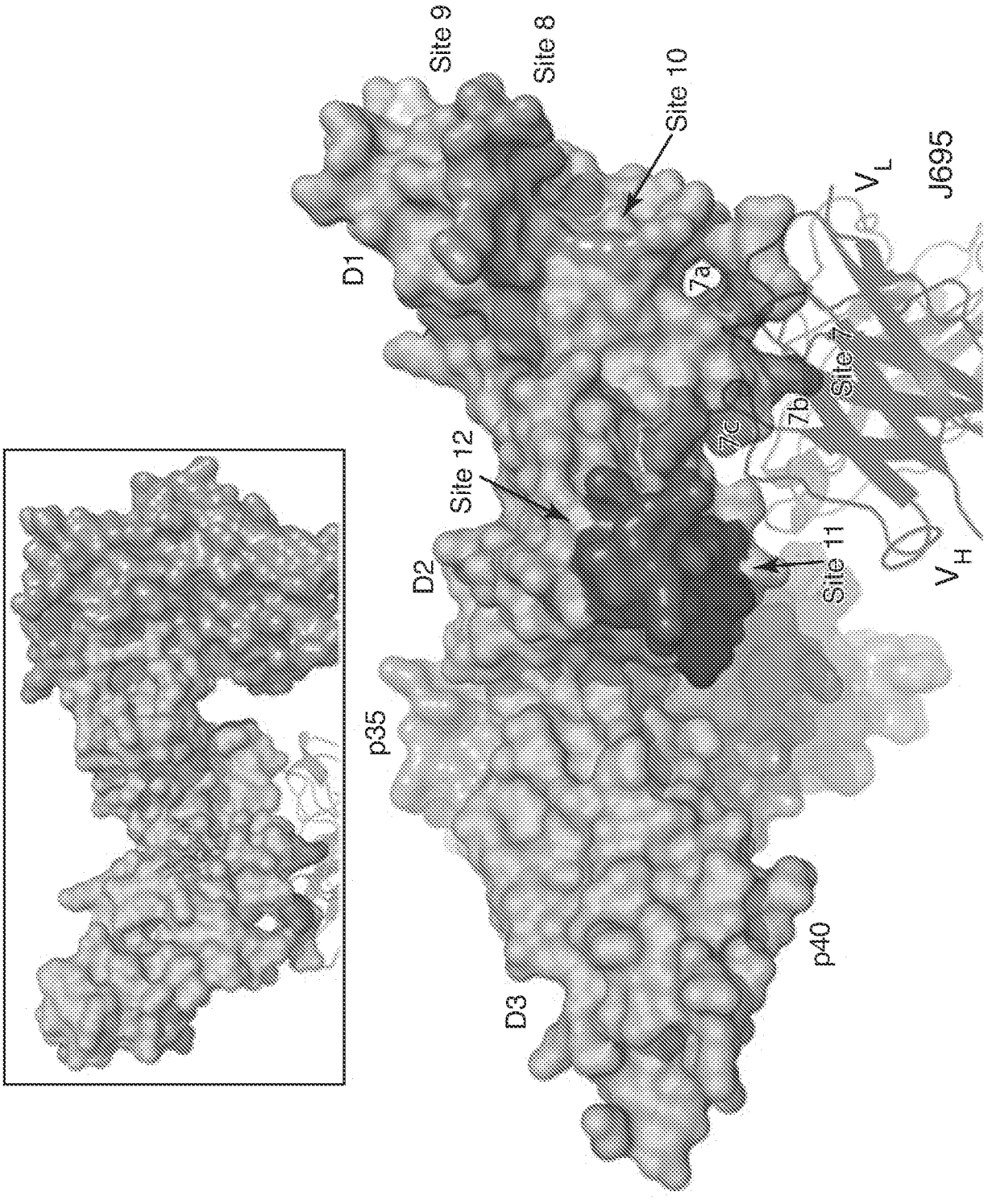

Site 9
Site 8
Site 10
D1
7a
V_L
J695
Site 7
7b
7c
Site 12
D2
Site 11
V_H
p35
p40
D3

Fig. 12

Fig. 13


Site 9
Site 8
Site 10
D1
7a
V_L
J695
Site 7
7b
7c
Site 12
D2
Site 11
V_H
p35
p40
D3

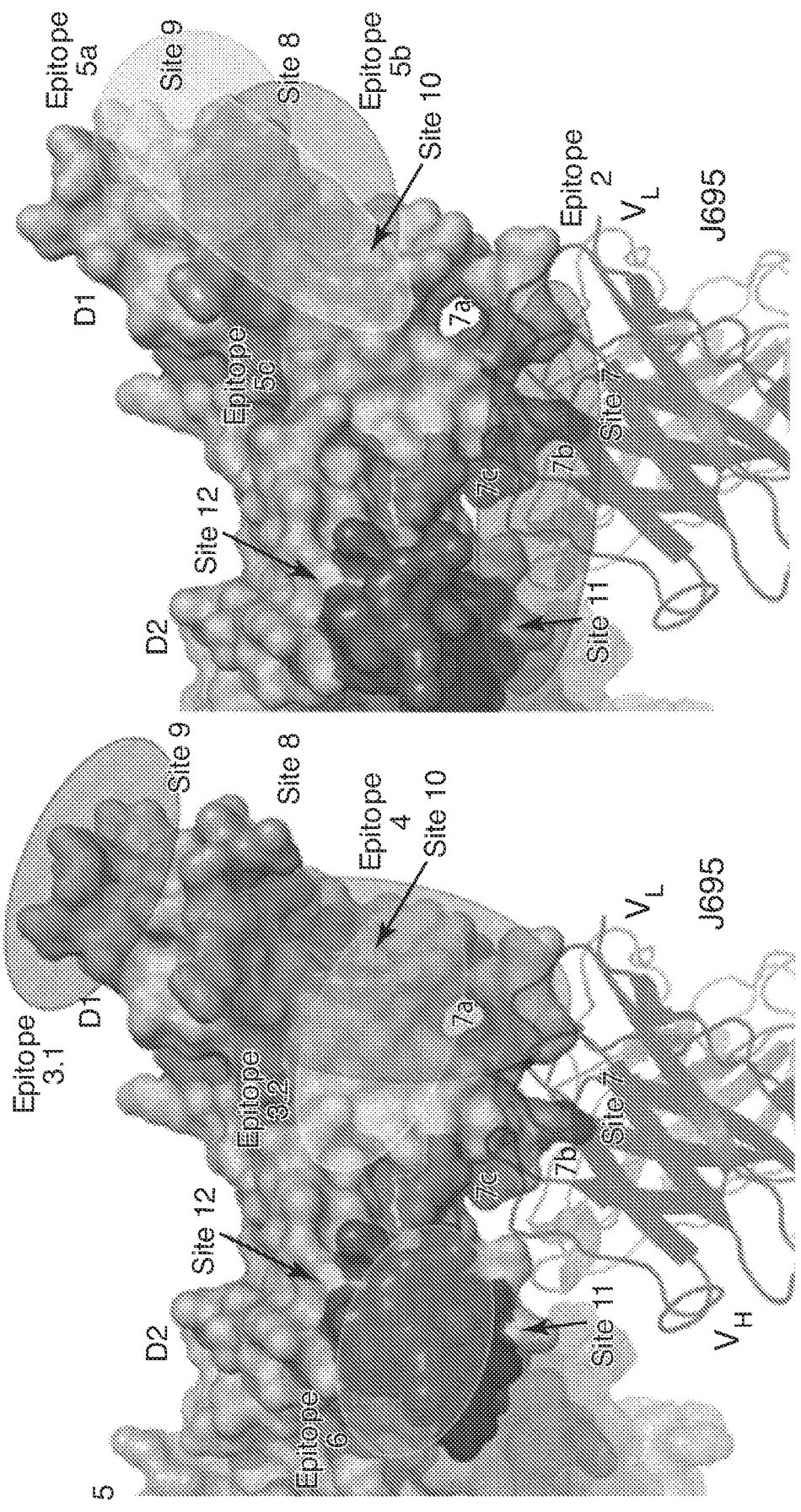

Epitope 5a
Site 9
Site 8
Epitope 5b
Site 10
Epitope 2
V_L
J695
D1
Epitope 5c
7a
Site 7
7b
7d
Site 12
D2
Site 11
Epitope 3.1
D1
Site 9
Site 8
Epitope 4
Site 10
V_L
J695
7a
Epitope 3.2
7c
7b
Site 7
Site 12
D2
Site 11
V_H
Epitope 6
5

Fig. 14

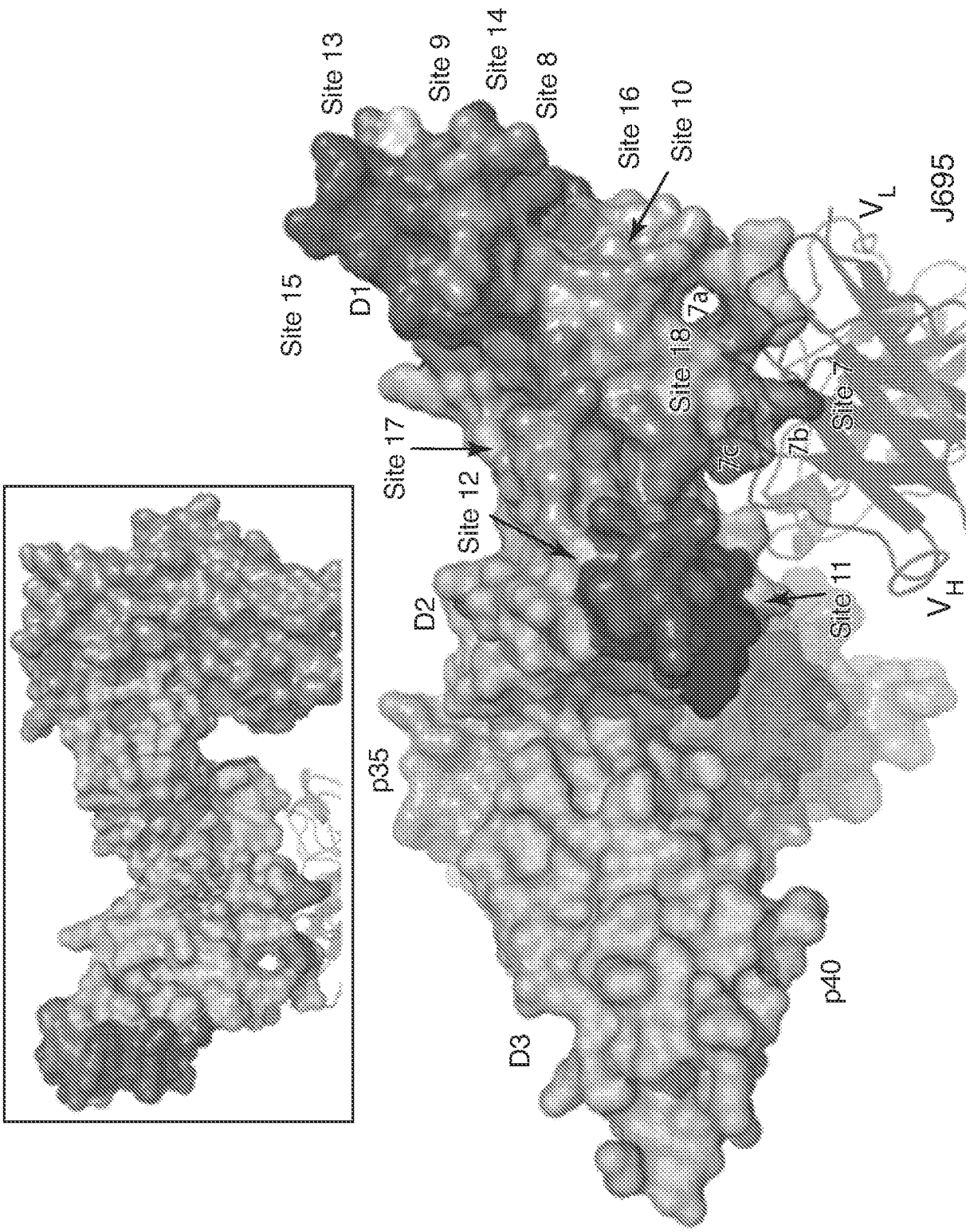

Site 13
Site 9
Site 14
Site 8
Site 16
Site 10
Site 15
D1
J695
V_L
7a
Site 18
Site 7
7c
7b
Site 17
Site 12
D2
Site 11
V_H
p35
p40
D3

Fig. 15